

PAMELA: Measurements of matter and antimatter in space

N. DE SIMONE⁽¹⁾⁽²⁾, G. JERSE⁽³⁾, E. MOCCHIUTTI^{(3)(*)}, O. ADRIANI⁽⁴⁾⁽⁵⁾,
G. C. BARBARINO⁽⁶⁾⁽⁷⁾, G. A. BAZILEVSKAYA⁽⁸⁾, R. BELLOTTI⁽⁹⁾⁽¹⁰⁾, M. BOEZIO⁽³⁾,
E. A. BOGOMOLOV⁽¹¹⁾, L. BONECHI⁽⁴⁾⁽⁵⁾, M. BONGI⁽⁵⁾, V. BONVICINI⁽³⁾,
S. BORISOV⁽¹⁾⁽¹²⁾, S. BOTTAI⁽⁵⁾, A. BRUNO⁽⁹⁾⁽¹⁰⁾, F. CAFAGNA⁽⁹⁾, D. CAMPANA⁽⁷⁾,
R. CARBONE⁽⁷⁾⁽²⁾, P. CARLSON⁽¹³⁾, M. CASOLINO⁽¹⁾, G. CASTELLINI⁽¹⁴⁾,
L. CONSIGLIO⁽⁷⁾, M. P. DEPASCALE⁽¹⁾⁽²⁾, C. DE SANTIS⁽¹⁾, V. DI FELICE⁽¹⁾⁽²⁾,
A. M. GALPER⁽¹²⁾, W. GILLARD⁽¹³⁾, L. GRISHANTSEVA⁽¹²⁾, A. V. KARELIN⁽¹²⁾,
S. V. KOLDASHOV⁽¹²⁾, S. Y. KRUTKOV⁽¹¹⁾, A. N. KVASHNIN⁽⁸⁾, A. LEONOV⁽¹²⁾,
O. MAKUMOV⁽⁸⁾, V. MALAKHOV⁽¹²⁾, V. MALVEZZI⁽¹⁾, L. MARCELLI⁽¹⁾,
A. G. MAYOROV⁽¹²⁾, W. MENN⁽¹⁵⁾, A. MONACO⁽⁹⁾⁽¹⁰⁾, V. V. MIKHAILOV⁽¹²⁾,
N. MORI⁽⁵⁾, N. N. NIKONOV⁽¹⁾⁽¹¹⁾, G. OSTERIA⁽⁷⁾, F. PALMA⁽¹⁾⁽²⁾, P. PAPINI⁽⁵⁾,
M. PEARCE⁽¹³⁾, P. PICOZZA⁽¹⁾⁽²⁾, C. PIZZOLOTTO⁽³⁾, M. RICCI⁽¹⁶⁾,
S. B. RICCIARINI⁽⁵⁾, L. ROSSETTO⁽¹³⁾, M. RUNTZO⁽¹²⁾, R. SARKAR⁽³⁾, M. SIMON⁽¹⁵⁾,
R. SPARVOLI⁽¹⁾⁽²⁾, P. SPILLANTINI⁽⁴⁾⁽⁵⁾, Y. I. STOZHKOVA⁽⁸⁾, A. VACCHI⁽³⁾,
E. VANNUCCINI⁽⁵⁾, G. VASILYEV⁽¹¹⁾, S. A. VORONOV⁽¹²⁾, J. WU⁽¹³⁾,
Y. T. YURKIN⁽¹²⁾, G. ZAMPA⁽³⁾, N. ZAMPA⁽³⁾ and V. G. ZVEREV⁽¹²⁾

⁽¹⁾ INFN, Sezione di Roma "Tor Vergata" - Via della Ricerca Scientifica 1
I-00133 Rome, Italy

⁽²⁾ Dipartimento di Fisica, Università di Roma "Tor Vergata" - Via della Ricerca Scientifica 1
I-00133 Rome, Italy

⁽³⁾ INFN, Sezione di Trieste - Padriciano 99, I-34149 Trieste, Italy

⁽⁴⁾ Dipartimento di Fisica, Università di Firenze - Via Sansone 1, I-50019 Sesto Fiorentino
(Firenze), Italy

⁽⁵⁾ INFN, Sezione di Firenze - Via Sansone 1, I-50019 Sesto Fiorentino (Firenze), Italy

⁽⁶⁾ Dipartimento di Fisica, Università di Napoli "Federico II" - Via Cintia
I-80126 Napoli, Italy

⁽⁷⁾ INFN, Sezione di Napoli - Via Cintia, I-80126 Naples, Italy

⁽⁸⁾ Lebedev Physical Institute - Leninsky Prospekt 53, RU-119991 Moscow, Russia

⁽⁹⁾ Dipartimento di Fisica, Università di Bari - Via Amendola 173, I-70126 Bari, Italy

⁽¹⁰⁾ INFN, Sezione di Bari - Via Amendola 173, I-70126 Bari, Italy

⁽¹¹⁾ Ioffe Physical Technical Institute - Polytekhnicheskaya 26, RU-194021
St. Petersburg, Russia

⁽¹²⁾ Moscow Engineering and Physics Institute - Kashirskoe Shosse 31
RU-11540 Moscow, Russia

⁽¹³⁾ KTH, Department of Physics, and the Oskar Klein Centre for Cosmoparticle Physics
AlbaNova University Centre - SE-10691 Stockholm, Sweden

⁽¹⁴⁾ IFAC - Via Madonna del Piano 10, I-50019 Sesto Fiorentino (Firenze), Italy

⁽¹⁵⁾ Universität Siegen - D-57068 Siegen, Germany

⁽¹⁶⁾ INFN, Laboratori Nazionali di Frascati - Via Enrico Fermi 40, I-00044 Frascati, Italy

(ricevuto il 25 Febbraio 2011; pubblicato online il 26 Aprile 2011)

(*) E-mail: Emiliano.Mocchiutti@ts.infn.it

Summary. — On the 15th of June 2006, the PAMELA satellite-borne experiment was launched from the Baikonur cosmodrome and it has been collecting data since July 2006. The apparatus comprises a time-of-flight system, a silicon-microstrip magnetic spectrometer, a silicon-tungsten electromagnetic calorimeter, an antineutrino system, a shower tail counter scintillator and a neutron detector. The combination of these devices allows precision studies of the charged cosmic radiation to be conducted over a wide energy range (100 MeV–100's GeV) with high statistics. The primary scientific goal is the measurement of the antiproton and positron energy spectra in order to search for exotic sources, such as dark matter particle annihilations. PAMELA is also searching for primordial antinuclei (anti-helium), and testing cosmic-ray propagation models through precise measurements of the antiparticle energy spectrum and precision studies of light nuclei and their isotopes. Moreover, PAMELA investigates phenomena connected with solar and earth physics. The main results and updated data will be presented.

PACS 98.70.Sa – Cosmic rays (including sources, origin, acceleration, and interactions).

PACS 96.50.sb – Composition, energy spectra and interactions.

PACS 07.87.+v – Spaceborne and space research instruments, apparatus, and components (satellites, space vehicles, etc.).

1. – Introduction

PAMELA is a dedicated satellite-borne experiment conceived by the WiZard Collaboration to study the anti-particle component of the cosmic radiation. In this work we describe the scientific objectives, the detector and the preliminary results of PAMELA after three years of data taking.

2. – Physics goals and instrument description

The PAMELA physics goal is the precise measurement of the cosmic ray composition at 1 Astronomical Unit (AU). Its 70 degrees, 350–610 km quasi-polar elliptical orbit makes it particularly suited to study items of galactic, heliospheric and trapped nature. PAMELA has been mainly conceived to perform high-precision spectral measurement of antiprotons and positrons and to search for antinuclei, over a wide energy range. Besides the study of cosmic antimatter, the instrument setup and the flight characteristics allow many additional scientific goals to be pursued [1].

The instrument is installed inside a pressurized container (2 mm aluminum window) attached to the Russian Resurs-DK1 Earth-observation satellite that was launched into the Earth orbit by a Soyuz-U rocket on June 15th 2006 from the Baikonur cosmodrome in Kazakhstan. The mission is foreseen to last till at least December 2011.

PAMELA was first switched on June 21st 2006 and it has been collecting data continuously since July 11th 2006. To date about 1230 days of data have been analyzed, corresponding to more than one billion recorded triggers and more than 18 TB data.

A schematic overview of the PAMELA apparatus is shown in fig. 1. The apparatus is ~ 1.3 m high, has a total mass of 470 kg and an average power consumption of 355 W. It comprises the following subdetectors, arranged as shown in figure (from top to bottom):

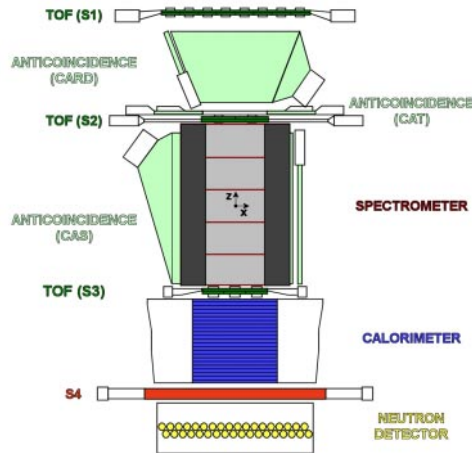


Fig. 1. – A schematic view of the PAMELA apparatus. The instrument is ~ 1.3 m high and has a mass of 470 kg. The average power consumption is 355 W. Magnetic field lines are oriented parallel to the y direction.

a time-of-flight system (TOF—S1, S2, S3); a magnetic spectrometer; an anticoincidence system (AC—CARD, CAT, CAS); an electromagnetic imaging calorimeter; a shower tail catcher scintillator (S4) and a neutron detector.

Planes of plastic scintillator mounted above and below the spectrometer form the TOF system. Its timing resolution allows albedo-particle identification and mass discrimination below $1 \text{ GeV}/c$. The TOF provides also a fast signal for triggering the data acquisition.

The central components of PAMELA are a permanent magnet and a tracking system composed of six planes of double-sided silicon sensors, which form the magnetic spectrometer. This device is used to determine the rigidity (momentum divided by charge) and the charge of particles crossing the magnetic cavity. The rigidity measurement is done through the reconstruction of the trajectory based on the impact points on the tracking planes and the resulting determination of the curvature due to the Lorentz force. The direction of bending of the particle (*i.e.* the discrimination of the charge sign) is the key method used to separate matter from anti-matter. The magnetic field of the spectrometer of PAMELA is generated by a permanent magnet composed of five identical modules placed one on top of another to form a 43.6 cm high tower. The acceptance of the spectrometer, which also defines the overall acceptance of the PAMELA experiment, is $21.5 \text{ cm}^2 \text{ sr}$ and the spatial resolution of the tracking system is better than $4 \mu\text{m}$ up to a zenith angle of 10° , corresponding to a maximum detectable rigidity exceeding 1 TV.

The spectrometer is surrounded by a plastic scintillator veto shield, aiming to identify false triggers and multiparticle events generated by secondary particles produced in the apparatus. Additional information to reject multiparticle events comes from the segmentation of the TOF planes in adjacent paddles and from the tracking system.

The main task of the electromagnetic calorimeter (16.3 radiation lengths, 0.6 interaction lengths) mounted below the spectrometer is to select positrons and antiprotons from the large background constituted by protons and electrons, respectively. Positrons have to be identified from a background of protons that is about 10^3 times the positrons component at $1 \text{ GeV}/c$, increasing to 5×10^3 at $10 \text{ GeV}/c$. Antiprotons have to be selected

from a background of electrons that decreases from 5×10^3 times the antiproton component at $1 \text{ GeV}/c$ to less than 10^2 times above $10 \text{ GeV}/c$. This means that PAMELA must be able to separate electrons from hadrons at a level better than 10^5 . Much of this rejection power in PAMELA is provided by the calorimeter. Besides the electron-hadron separation, the calorimeter directly measures the energy of electrons and positrons. The sampling imaging calorimeter comprises 44 single-sided silicon strip detector planes interleaved with 22 plates of tungsten absorber. The high granularity of the calorimeter and the use of silicon strip detectors provide detailed information on the longitudinal and lateral profiles of particles' interactions as well as a measure of the deposited energy.

A plastic scintillator system mounted beneath the calorimeter aids the identification of high-energy electrons and is followed by a neutron detection system for the selection of high-energy electrons which shower in the calorimeter. More technical details about the entire PAMELA instrument and launch preparations can be found in [2].

3. – Anti-particle measurement

The main task of PAMELA is to measure the antimatter components of the cosmic-ray. At high energy, main sources of background in the antimatter samples result from spillover (protons in the antiproton sample and electrons in the positron sample) and from like-charged particles (electrons in the antiproton sample and protons in the positron sample). Spillover background originates from the wrong determination of the charge sign due to measured deflection uncertainty; its extent is related to the spectrometer performances and its effect is to set a limit to the maximum rigidity up to which the measurement can be extended. The like-charged particle background is related to the capability of the instrument to perform electron-hadron separation.

3.1. Antiproton-to-proton ratio. – Electrons in the antiproton sample can be easily rejected by applying conditions to the calorimeter shower topology, while the main source of background originates from spillover protons. In order to reduce the spillover background and accurately measure antiprotons up to the highest possible energy, strict selection criteria were imposed on the quality of the fit. To measure the antiproton-to-proton flux ratio the different calorimeter selection efficiencies for antiprotons and protons were estimated. The difference is due to the momentum-dependent interaction cross-sections for the two particles. These efficiencies were studied using both simulated antiprotons and protons, and proton samples selected from the flight data. In this way it was possible to normalize the simulated proton and therefore the antiproton selection efficiency.

The left panel of fig. 2 shows the antiproton-to-proton flux ratio measured by the PAMELA experiment [3, 4] compared with other recent measurements [5-9]. Only statistical errors are shown since the systematic uncertainty is less than a few percent of the signal, which is significantly lower than the statistical uncertainty. The PAMELA data are in excellent agreement with recent data from other experiments, the antiproton-to-proton flux ratio increases smoothly with energy up to about 10 GeV and then levels off. The data follow the trend expected from secondary production calculations and our results are sufficiently precise to place tight constraints on secondary production calculations and contributions from exotic sources [4].

3.2. Positron fraction. – Protons are the main source of background in the positron sample and an excellent positron identification is needed to reduce the contamination at a negligible level.

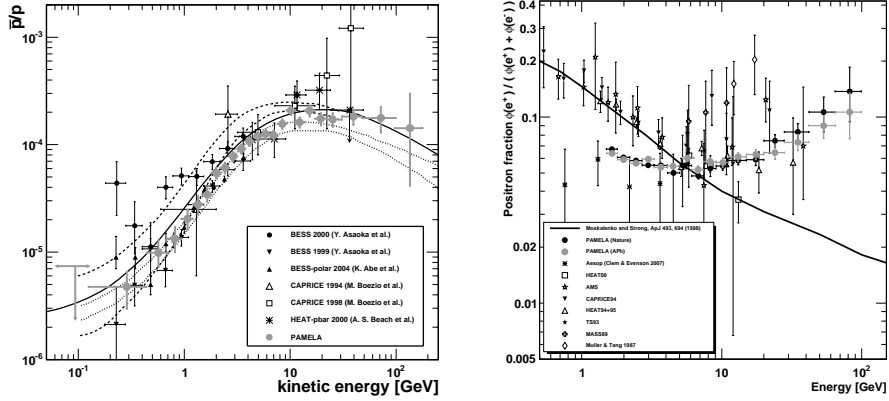


Fig. 2. – Left panel: the antiproton-to-proton flux ratio obtained by PAMELA compared with recent measurements. Right panel: the PAMELA positron fraction compared to other experimental results and the standard model prediction for secondary positron production.

The method used to obtain the published results is the proton background estimation method. This approach consists in keeping a very high selection efficiency and in quantifying the residual proton contamination by means of a so-called “spectral analysis” [10,11]. In a conservative approach, the proton distributions needed to estimate the contamination were obtained using the flight calorimeter data without any dependence on simulations or test beam data. The calorimeter was divided in two parts: the upper part (“pre-sampler”) made of two tungsten planes and four detector planes was used to reject non-interacting particles. The sample of events passing this condition is a nearly pure sample of protons with a positron contamination of less than 2% at rigidities greater than 1.5 GV. Calorimeter variables were evaluated for the lower part of the calorimeter made of 20 tungsten planes and 40 detector planes and the distribution of the lateral shower spread for protons was obtained. Hence, positive particles were selected using the first 20 tungsten planes of the calorimeter. Results are shown in the right panel of fig. 2 where PAMELA data [10,11] are compared to some recent measurements [12-20] and to the standard model theoretical prediction for secondary positron production. At low energy PAMELA data are lower than most of the other data and this can be interpreted as an observation of charge-sign-dependent solar modulation effects. Between about 6 and 10 GeV the PAMELA positron fraction is compatible with other measurements and above 10 GeV it increases significantly with energy. The PAMELA data cannot be described by the standard model of secondary production, black line in fig. 2, right panel. The secondary production model has its indetermination due to the knowledge of the fluxes of primary particles, of the interaction cross-sections, of the average amount of traversed matter, and of the electron spectrum. However the rising at $E > 10$ GeV seems a very difficult feature to be reproduced by a pure secondary component without using an unrealistic soft electron spectrum and *ad hoc* tuning of the other parameters [21], suggesting the existence of other primary sources [22].

Many explanations about the origin of the positron excess have been postulated. These models can be divided in terms of astrophysical sources, like pulsars [23] or the distribution of Supernovae remnants [24] in the Galaxy, or more speculative ones, like annihilation of new type of dark matter [25] or of the lightest superparticle dark matter [26].

4. – Particle measurements

The measurement of standard particles (protons, nuclei and electrons) in the cosmic radiation is easier respect to the anti-particle measurements due to their abundance. Hence the sample selection is usually very efficient and the main effort must be put in the study of any possible systematic uncertainty.

4.1. Protons and helium nuclei spectra. – Protons and helium nuclei are the most abundant components of the cosmic radiation. Precise measurements of their fluxes are needed to understand the acceleration and subsequent propagation of cosmic rays in the Galaxy. The results reported by PAMELA [27] in the rigidity range 1 GV–1.2 TV show that the spectral shapes of these two species are different and cannot be well described by a single power law. These data challenge the current paradigm of cosmic-ray acceleration in supernova remnants followed by diffusive propagation in the Galaxy. More complex processes of acceleration and propagation of cosmic rays are required to explain the spectral structures observed.

4.2. Negative electron spectrum. – As discussed previously, the positron fraction rise measured by PAMELA could be due to a very soft electron (e^-) spectrum. It is therefore important to precisely measure the negative electron spectrum in order to put a constraint in the interpretation of the positron fraction rise. Moreover, if a primary positron source exists, it is difficult to explain the generation and acceleration of positrons without generating and accelerating the same amount of electrons. This implies that a negative electron spectrum measurement with high enough statistic and precision should reveal spectral features in the same energy range at which the positron fraction seems to deviate from the expected background.

The PAMELA apparatus is able to separate negative electrons from positrons up to about 600 GeV [28]. The capabilities of the PAMELA detector allow also any systematic effect due to the energy measurement to be minimized and estimated. In fact the energy of electrons can be determined using two independent detectors: the spectrometer and the electromagnetic calorimeter. Figure 3 shows the negative electron spectrum as measured by PAMELA. Both the presented fluxes have been obtained selecting negative particles with the spectrometer; the energy measurement and binning is different and is performed using the tracking system (full circles) or the calorimeter (open circles). In the case of the calorimeter energy determination, in order to minimize the transversal leakage, strong containment conditions are required. This reduces the statistics of the sample. Longitudinal leakage is taken into account by fitting the shower longitudinal profile with a gamma function. With these conditions a precise energy measurement is achieved.

As can be seen from the figure, the resulting fluxes are in very good agreement and the comparison between the two fluxes can be used to set a 2% systematic error in the negative electron spectrum measurement.

Although the overall results can be easily described by a single power law, a certain hardening of the spectrum may be present at high energies. This interesting feature seems to be in agreement with the positron fraction measurement.

4.3. Nuclei. – Light nuclei up to oxygen are detectable with the dE/dx measured by the scintillator of the TOF system. It is possible to study with high statistics the secondary/primary cosmic ray nuclear and isotopic abundances such as B/C, Be/C, Li/C and $^3\text{He}/^4\text{He}$. These measurements can be used to tune existing production and propagation models in the galaxy, providing detailed information on the galactic structure

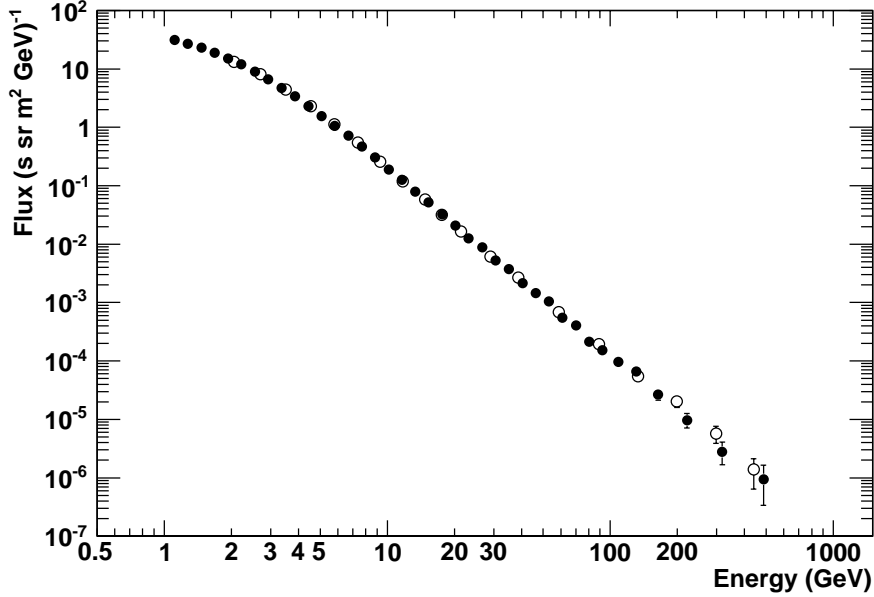


Fig. 3. – Electron flux as measured with PAMELA: comparison between the energy spectrum obtained using the spectrometer (closed circles) and the same using the calorimeter (open circles) to determine the energy of the events.

and the various mechanisms involved. The preliminary B/C ratio as a function of kinetic energy per nucleon measured by PAMELA is in good agreement with previous measurements.

5. – Other measurements

5.1. Solar modulation galactic cosmic rays. – Since protons and helium nuclei are detected by PAMELA with very high statistics it is possible to precisely study time variations and transient phenomena during the present 23rd solar minimum.

A long-term measurement of the proton, electron and nuclear flux at 1 AU provides information on propagation phenomena occurring in the heliosphere. As already mentioned, the possibility to measure the anti-particle spectra allow also charge-dependent solar modulation effects to be studied. The proton flux as measured by PAMELA in different time intervals shows an increasing flux of galactic cosmic rays corresponding to a decreasing solar activity. This effect is in agreement with the increase in the fluxes as measured by neutron monitors at ground [29].

5.2. Re-entrant albedo and trapped particles measurements. – Albedo particles are secondary particles produced by cosmic rays interacting with the Earth's atmosphere that are scattered upward. When these particles lack sufficient energy to leave the Earth's magnetic field they re-enter the atmosphere in the opposite hemisphere but at a similar magnetic latitude and they are called re-entrant albedo particles. The measurement of the composition and spectra of the secondary cosmic rays particles provides a tool for the

fine tuning of models used in air shower simulation programs. Due to its orbit PAMELA is able to provide a world map of the primary and re-entrant albedo particles, allowing fine details in the spectra, especially in the sub-cutoff region, to be discerned. It is, in fact, possible to observe structures in the spectra in the sub-cutoff region which are also reproduced by simulations [30].

The 70° orbit of the Resurs-DK1 satellite allows for continuous monitoring of the electron and proton belts. The high energy (> 80 MeV) component of Van Allen Belts can be monitored during the time and it is possible to perform a detailed mapping of these regions [31].

5.3. Solar energetic particles. – Due to the period of solar minimum few significant solar events with energy high enough to be detectable are expected. The observation of solar energetic particle (SEP) events with a magnetic spectrometer permits several aspects of solar and heliospheric cosmic ray physics to be addressed for the first time. PAMELA detected the December 2006 SEP event and results will soon be published.

6. – Conclusions

PAMELA is continuously taking data and the mission is planned to continue until at least December 2011. The increase in statistics will allow higher energies to be studied. An analysis for positron flux till low energy (down to 100 MeV), and primary cosmic rays nuclei is in progress and will be the topic of future publications.

* * *

We would like to acknowledge contributions and support from: Italian Space Agency (ASI), Deutsches Zentrum für Luft- und Raumfahrt (DLR), The Swedish National Space Board, Swedish Research Council, Russian Space Agency (Roskosmos, RKA). R. S. wishes to thank the TRIL program of the International Center of Theoretical Physics, Trieste, Italy that partly sponsored his activity.

REFERENCES

- [1] PICOZZA P. *et al.*, *Proceedings of 20th ECRS, Lisbon – Portugal 2006*, electronic version only, available at <http://www.lip.pt/events/2006/ecrs/proc/>.
- [2] PICOZZA P. *et al.*, *Astrophys. J.*, **27** (2007) 296.
- [3] ADRIANI O. *et al.*, *Phys. Rev. Lett.*, **102** (2009) 051101.
- [4] ADRIANI O. *et al.*, *Phys. Rev. Lett.*, **105** (2010) 121101.
- [5] BOEZIO M. *et al.*, *Astrophys. J.*, **561** (2001) 787.
- [6] BEACH A. S. *et al.*, *Phys. Rev. Lett.*, **87** (2001) 271101.
- [7] BOEZIO M. *et al.*, *Astrophys. J.*, **487** (1997) 415.
- [8] ASAOKA Y. *et al.*, *Phys. Rev. Lett.*, **88** (2002) 051101.
- [9] ABE K. *et al.*, *Phys. Lett. B*, **670** (2008) 103.
- [10] ADRIANI O. *et al.*, *Nature*, **458** (2009) 607.
- [11] ADRIANI O. *et al.*, *Astropart. Phys.*, **34** (2010) 1.
- [12] GOLDEN R. L. *et al.*, *Astrophys. J.*, **436** (1994) 769.
- [13] ALCARAZ J. *et al.*, *Phys. Lett. B*, **484** (2000) 10.
- [14] BEATTY J. J. *et al.*, *Phys. Rev. Lett.*, **93** (2004) 241102.
- [15] BARWICK S. W. *et al.*, *Astrophys. J.*, **482** (1997) L191.
- [16] GAST H., OLZEM J. and SCHAEEL S., *Proceedings of XLI Rencontres de Moriond, Electroweak Interaction and Unified Theories, La Thuile, Italy, 2006*, edited by TRESSE L., MAUROGORDATO S., TRAN THANH VAN J. (Edition Frontieres) 2006, p. 421.

- [17] BOEZIO M. *et al.*, *Astrophys. J.*, **532** (2000) 653.
- [18] CLEM J. and EVENSON P., *Proceedings of 30th International Cosmic Ray Conference, Merida – Mexico 2006*, Vol. **6**, edited by CABALLERO R., D’OLIVO J. C., MEDINA-TANCO G. and VALDÉS-GALICIA J. F. (Universidad Nacional Autónoma de México, Mexico City, Mexico) 2008, p. 27.
- [19] MÜLLER D. and TANG K. K., *Astrophys. J.*, **312** (1987) 183.
- [20] MOSKALENKO I. and STRONG A., *Astrophys. J.*, **493** (1998) 694.
- [21] DELAHAYE T., DONATO F., FORNENGO N., LAVALLE J., LINEROS R., SALATI P. and TAILLET R., astro-ph/0809.5268 preprint (2008).
- [22] SERPICO P. D., *Phys. Rev. D*, **79** (2009) 021302.
- [23] YUKSEL H., KISTLER M. D. and STANEV T., astro-ph/0810.2784 preprint (2008).
- [24] SHAVIV N. J., NAKAR E. and PIRAN T., astro-ph/0902.0376 preprint (2009).
- [25] HOOPER D. and PROFUMO S., *Phys. Rep.*, **453** (2007) 29.
- [26] GRAJEK P. *et al.*, astro-ph/0812.4555 preprint (2008).
- [27] ADRIANI O. *et al.*, *Science*, **332** (2011) 69.
- [28] ADRIANI O. *et al.*, submitted to *Phys. Rev. Lett.*, arXiv: astro-ph 1103.2880.
- [29] For example <http://neutronm.bartol.udel.edu/modplot.html>.
- [30] HONDA M. *et al.*, *Phys. Rev. D*, **70** (2004) 043008.
- [31] CASOLINO M. *et al.*, *J. Phys. Soc. Jpn.*, **78**, Suppl. A (2009) 35.